Supplemental Information

Parallel processing of sound dynamics across mouse auditory cortex via spatially patterned thalamic inputs and distinct areal intracortical circuits

Ji Liu, Matthew R. Whiteway, Alireza Sheikhattar, Daniel A. Butts, Behtash Babadi, Patrick O. Kanold*

9 Supplemental Figures

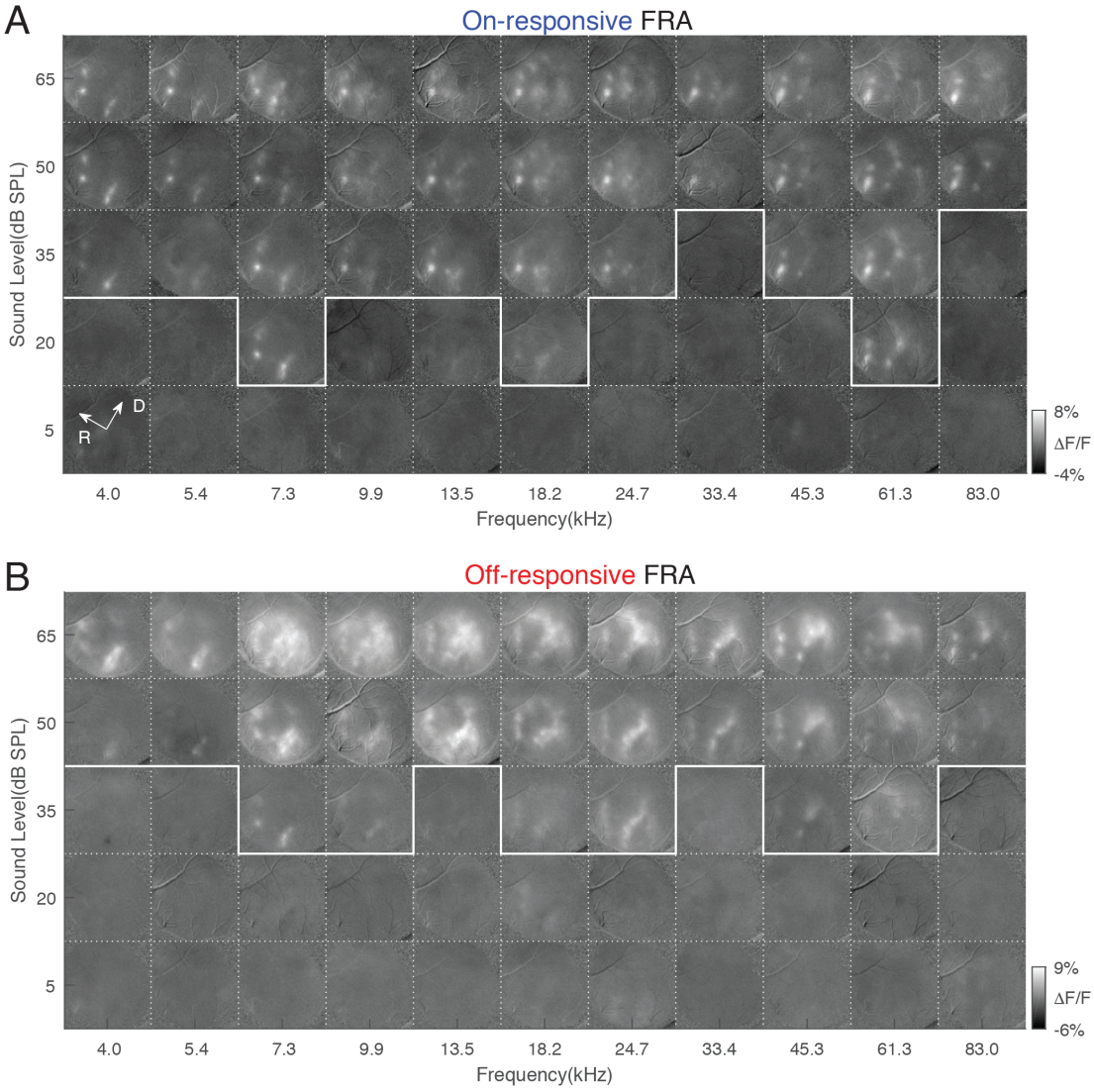

Figure S1. Related to Figure 1. Tone onset and offset differentially activate large areas of ACX.

(A) On-R frequency response area (FRA). Baseline subtracted average images within 200-500ms after tone onset are plotted as a function of frequency and sound level. White solid lines show threshold at each frequency. (B) Off-R FRA. Average images within 200-500ms after tone offset are plotted with images 0-200ms before tone offset used as baseline. Typically, Off-R had a higher threshold than On-R.

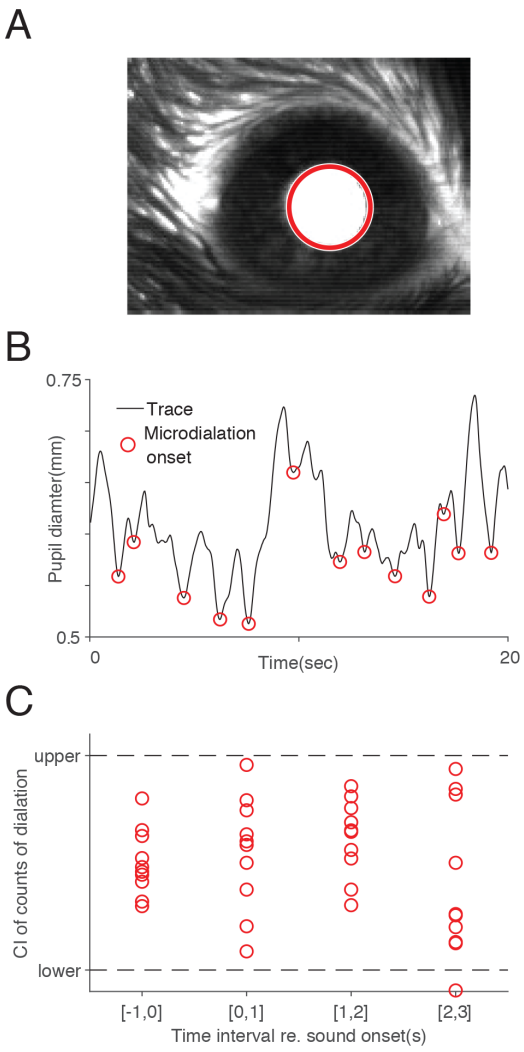

Figure S2. Related to Figure 1. On/Off-R is not related to the animal's arousal state

We presented the tones to passively listening animals, and it is possible that the sudden termination of the sound could change the arousal state of the animal and that this caused Off-Rs. To investigate this possibility, we monitored the state of the animal through pupillometry (McGinley et al., 2015) and quantified occurrence of pupil micro-dilation before, during and after tone presentation. Pupil dilation typically indicates increase in arousal state (Reimer et al., 2014). (A) Example pupillometry image and pupil size detection (red circle). (B) Example pupil diameter trace and micro-dilation onset detected with MATLAB built-in function 'findpeak' with a minimum

prominence of 10um. (C) Pupil dilation occurrence was quantified in four 1-second windows covering time before, during and after the tone presentation. The plot is normalized to the confidence interval computed through shuffling stimulus onset time. Most occurrence was well within the confidence interval, suggesting that pupil dilation happens equally likely before, during and after tone presentation and thus is unlikely to bias On-R or Off-R.

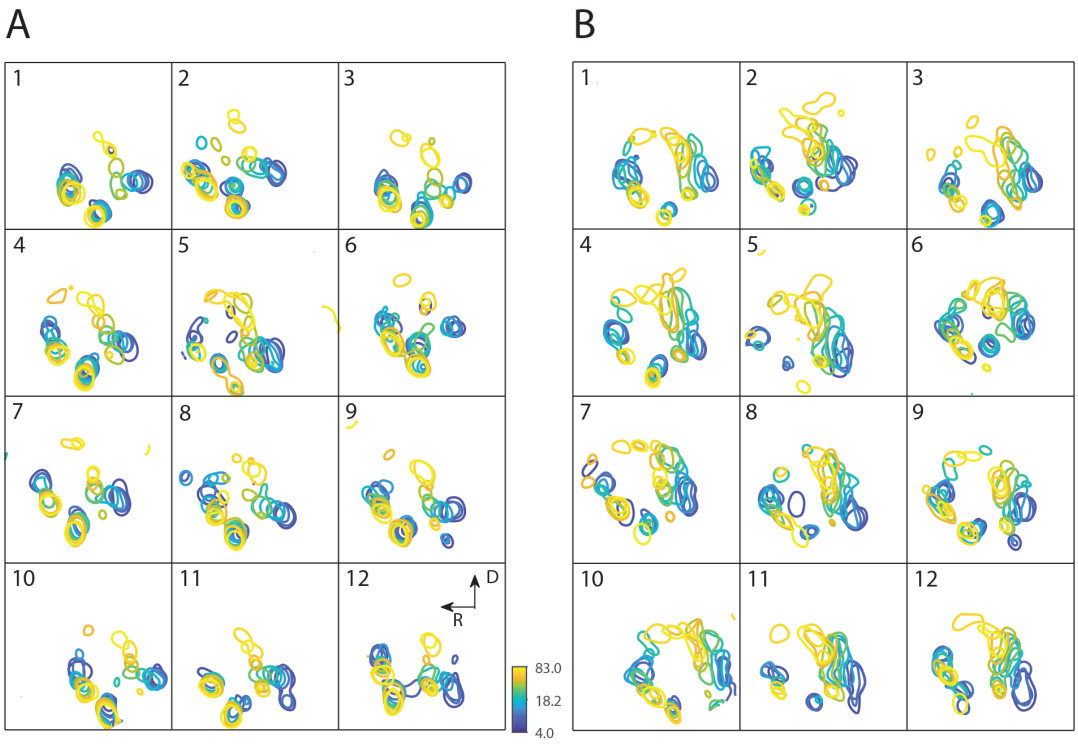

Figure S3. Related to Figure 1. ACX organization is stereotypical across mice.

On-tonotopy (A) and Off-tonotopy (B) of 12 other animals imaged. The colorbar indicates frequency of tones.

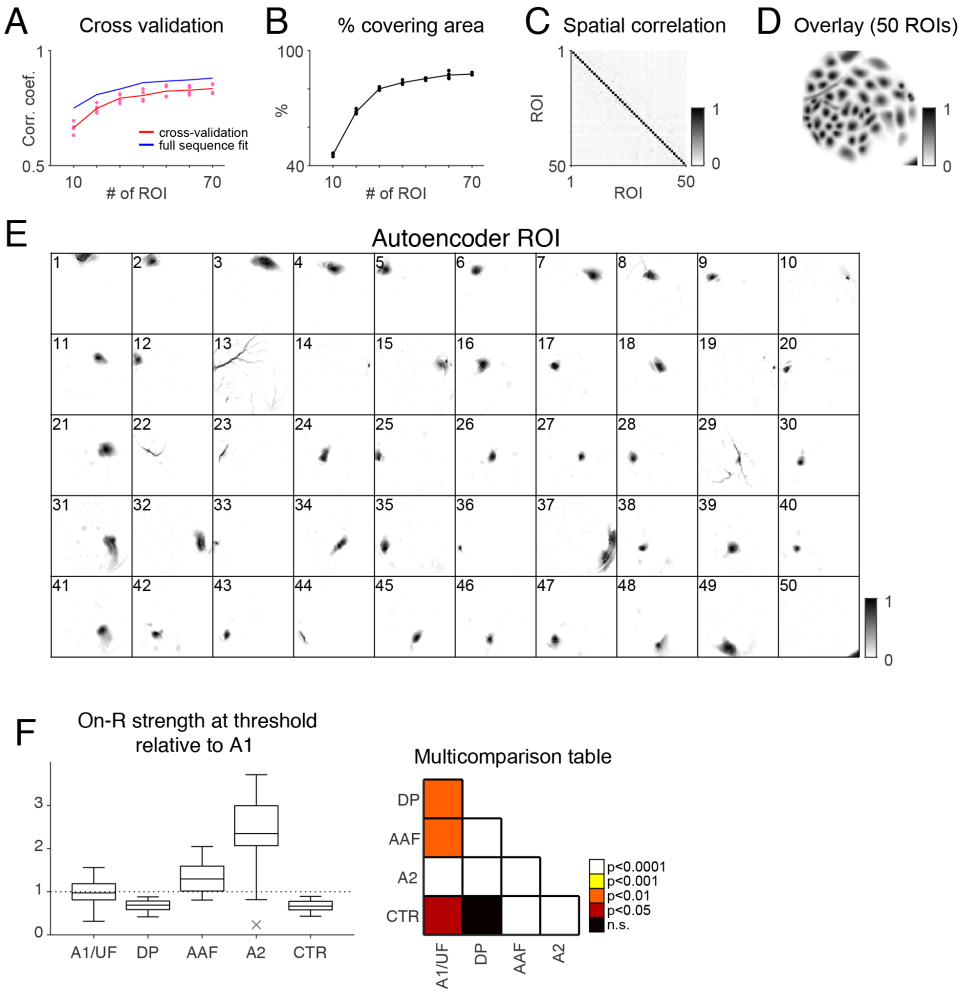

Figure S4. Related to Figure 2. Behavior of autoencoder fitting.

(A) Correlation with original image sequence obtained from cross-validation procedure and from full sequence fit as a function of ROI number. With 50 ROIs, the correlation value is around 0.8. (B) Areas covered by ROIs as a function of ROI number. (C) Spatial correlation of the 50 ROIs shown in (E). (D). Overlay of 50 ROIs. Note dense covering of cranial window. (E) Example of 50 ROIs shown individually. (F) The average On-R strength of parsed ACX fields normalized relative to A1 at the threshold. The right panel shows multi-comparison significance test performed on ANOVA statistics. DP and the center region ("CTR") had weak On-R at threshold.

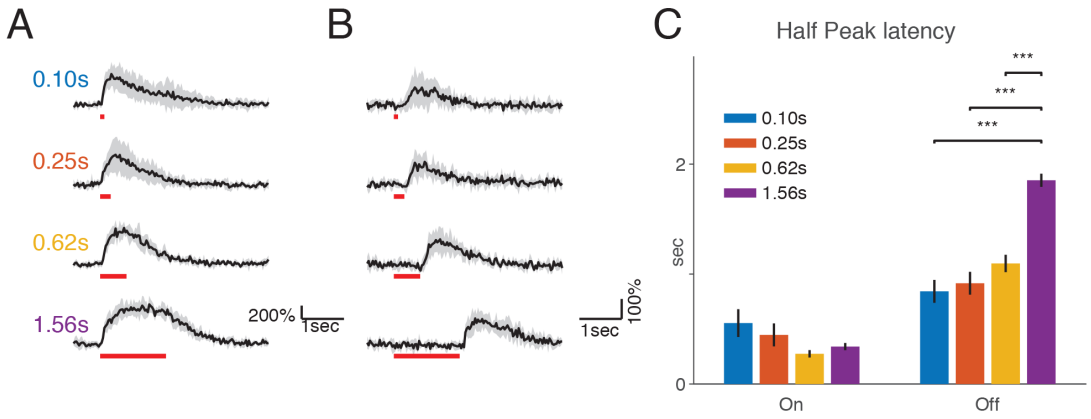

Figure S5. Related to Figure 4. Neuronal Off-R is time locked to tone offset.

Tones of different durations were presented to the same group of neurons and the offset-responses were time locked to tone offset and thus were not 'delayed' response happening at specific time point after tone onset. (A) Example On-responsive neuron responding to 0.10, 0.25, 0.62, 1.56 second tones. The response is time locked to tone onset. Red lines represent tone durations. (B) Example Off-responsive neuron whose responses were time locked to tone offset. (C) Time to reach half of maximum activation was quantified for On- and Off-R respectively. For On-R, the latency is not a function of tone duration while Off-R latency shifts systematically as a function of tone duration. '***' indicates $p<0.001$.

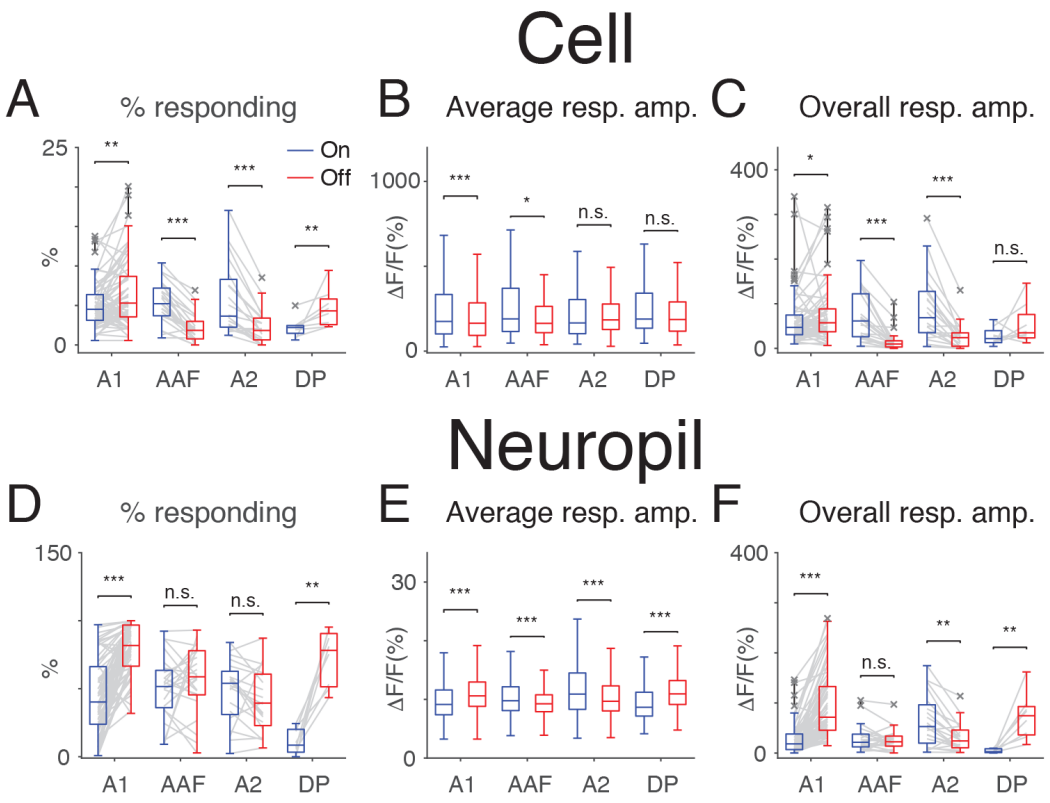

Figure S6. Related to Figure 4.

(A) Percentage of on-responding and off-responding neurons as a function auditory field. Each gray line represents a field of view. In A1 and DP, more cells responded to tone offset than to onset while the opposite was seen in AAF and A2. Paired t-test: A1, 6.62% ± 4.34% vs. 5.05% ± 2.89%, t(66)=-3.58, p=0.0007; AAF, 2.14% ± 1.83% vs. 5.36% ± 2.58, t(23) = 8.57, $p=1.29\times10^{-8}$); A2, 2.28% ± 2.24% vs. 5.83% ± 4.53%, t(19)=5.70, $p=1.7\times10^{-5}$; DP: 4.64% ± 2.42% vs. 2.23% ± 1.29%, t(7)=-2.50, p=0.041.Few neurons showed both On-Rs and Off-Rs (A1, 0.98% ± 0.90%; AAF, 0.54% ± 0.54%; A2, 0.95% ± 1.31%; DP 0.43% ± 0.57%). (B) Average On/Off-R amplitude of individual neurons was pooled over field of views and plotted as a function of auditory fields. The relative response amplitude for On-R and Off-R could vary across areas. Wilcoxon rank sum test, A1, z=3.34, $p=8\times10^{-4}$; AAF, z=2.34, p=0.0174; A2, z=-1.21, p=0.23; DP, z=1.14, p=0.26). (C) Overall cellular On/Off-R

amplitude (summing over all significant On-R or Off-Rs from all frequencies and all cells within a field of view) as a function of auditory field. The relative population composition and response amplitude well predicted the areal On/Off preferences on the large-scale (widefield). Wilcoxon signed rank test: A1, z=-2.30, p=0.0214; AAF, z=4.07, $p=4.6\times10^{-5}$; A2, z=3.73, $p=1.89\times10^{-4}$; DP, p=0.19. (D-F) Same as in (A-C) but plotted for neuropil. (D) Paired t-test: A1, t(66)=-10.4, $p=1.23\times10^{-15}$; AAF: t(23) = -1.12, p=0.27; A2: t(19)=1.51, p=0.15; DP, t(7)=-6.99, $p=2.14\times10^{-4}$. (E) Wilcoxon rank sum test, A1, z=-33, $p=1.62\times10^{-239}$; AAF: z=9.55, $p=1.32\times10^{-21}$; A2: z=9.67, $p=4.21\times10^{-22}$; DP, z=-10.1, $p=5.09\times10^{-24}$. (F) Wilcoxon rank sum test, A1, z=-7.61, $p=2.66\times10^{-14}$; AAF: z=0.01, p=0.99; A2: z=2.07, p=0.038; DP, $p=1.55\times10^{-4}$.

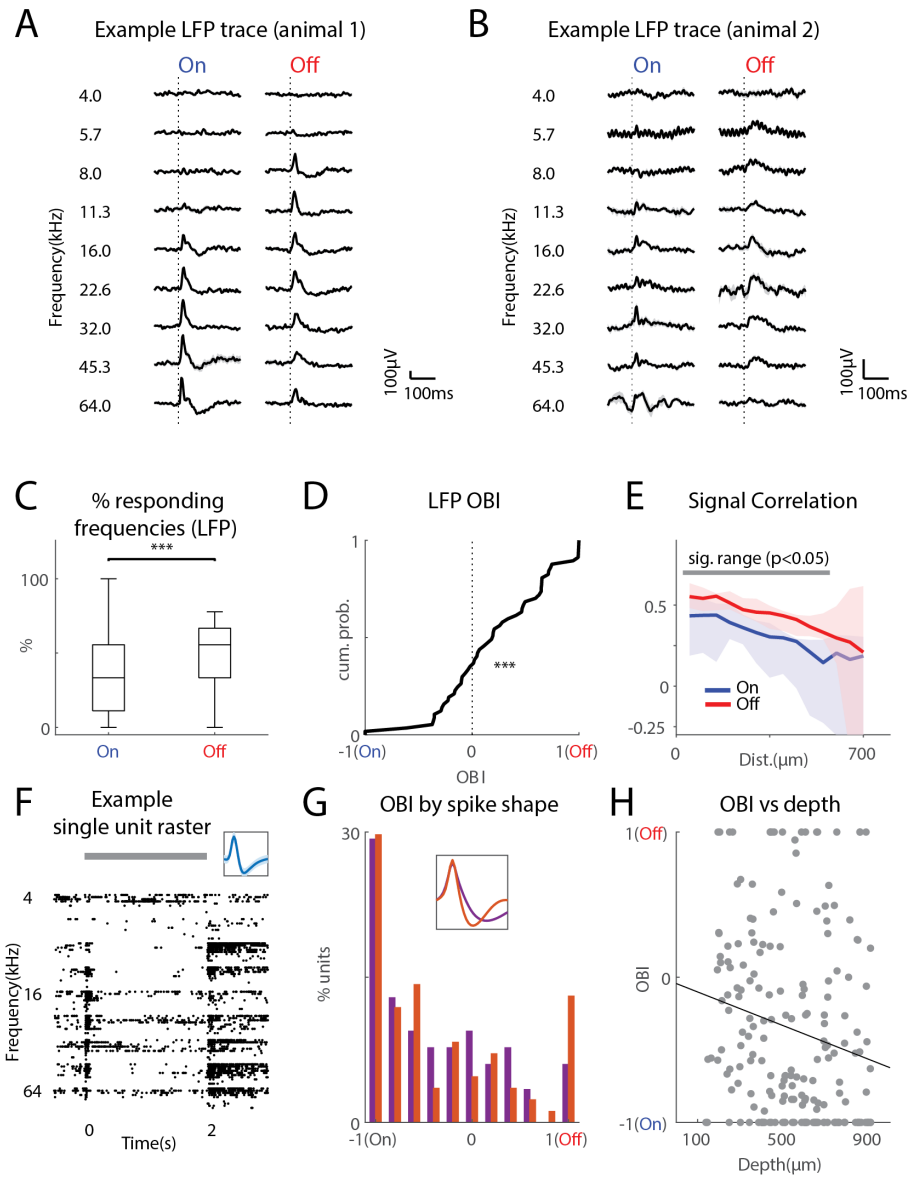

Figure S7. Related to Figure 4. Local field potential (LFP) in A1 shows bias towards Off-R in strength and spatial spread.

(A, B) Two example electrode contacts showing On- and Off-R to different tone frequencies. Dotted vertical lines represent tone onset and offset respectively. (C) Percentage of frequencies evoking significant On- or Off-R shows an Off-R bias in LFP responses (Wilcoxon signed-rank test, $p=9.5\times10^{-6}$). (D) LFP Off-R Bias Index (OBI) distribution is significantly shifted towards 1 (t-test, $p=3.6\times10^{-6}$), suggesting an overall larger Off-R. (E) Signal correlation (SC) was computed

for On- and Off-R separately among all electrode contacts and Off-R SC was larger than On-R SC over distance (Wilcoxon rank sum test, 50μm: p=0.040; 100μm: p=0.036; 150μm: p=0.038; 200μm: p=0.041; 250μm: p=0.023; 300μm: p=0.011; 350μm: p=0.008; 400μm: p=0.003; 450μm: p=0.003; 500μm: p=0.004; 550μm: p=0.034). (F) Example raster plot of one single unit responding to both tone onset and offset. The inset shows the spike waveform. (G) Histogram showing OBI separately for wide and narrow spike waveforms (putative excitatory and inhibitory neurons). Both groups show prominent On-R and the majority of the units had both On- and Off-R. (H) OBI of single units depended on cortical depth. A linear model was used to quantify the depth dependence of single unit OBI and deeper cortical layers were more biased towards On-R (linear fit: $y=-5.8\times10^{-4}*x-0.043$, $p=7.3\times10^{-3}$, adjusted $R^2=0.031$).

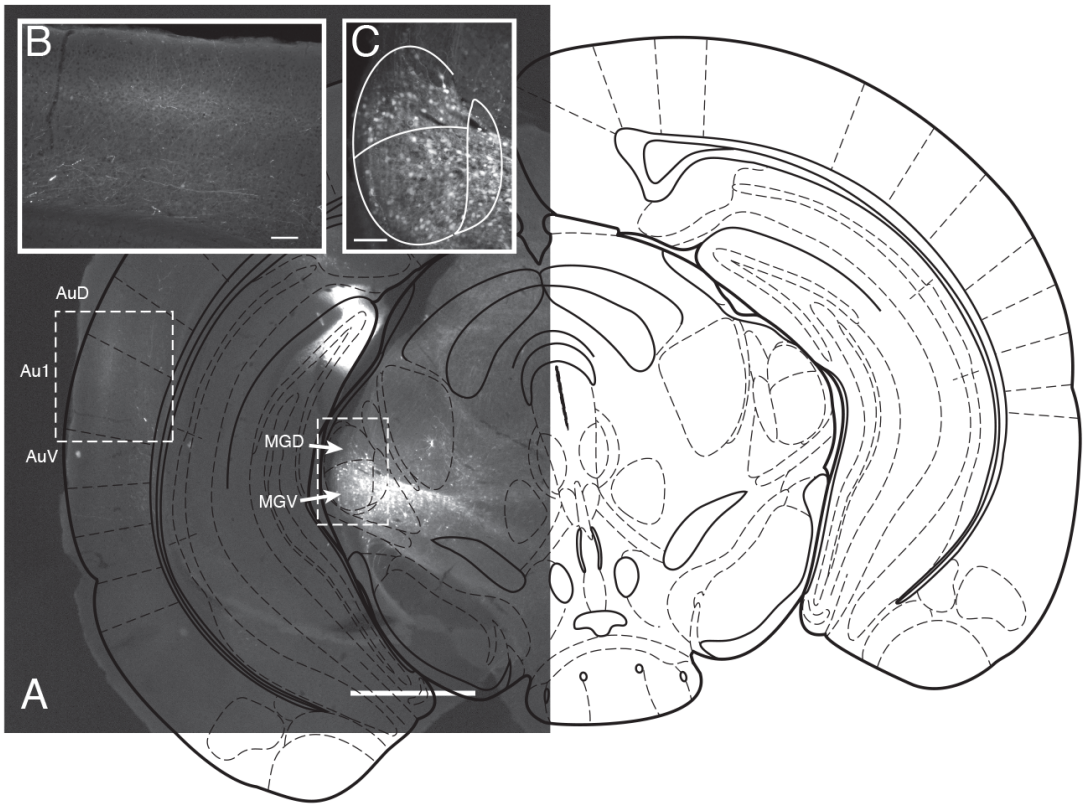

Figure S8. Related to Figure 6. MGB injections of AAV-GCAMP6s label terminals in A1

Viral injection of AAV1.hSyn1.mRuby2.GSG.P2A.GCaMP6s.WPRE.SV40 in MGB. mRuby signal was imaged. (A) Overall image of injection site and cortical terminals (2x). Scale bar shows 1mm. Labeling in hippocampus is due to injection tract. (B) 10x view of auditory cortex. Terminals can be seen in layer 4 and deeper layers, consistent with typical MGBv projection pattern. Scale bar shows 100μm. (C) 10x view of MGB. Labeled cells can be seen in all divisions. Scale bar shows 100μm.

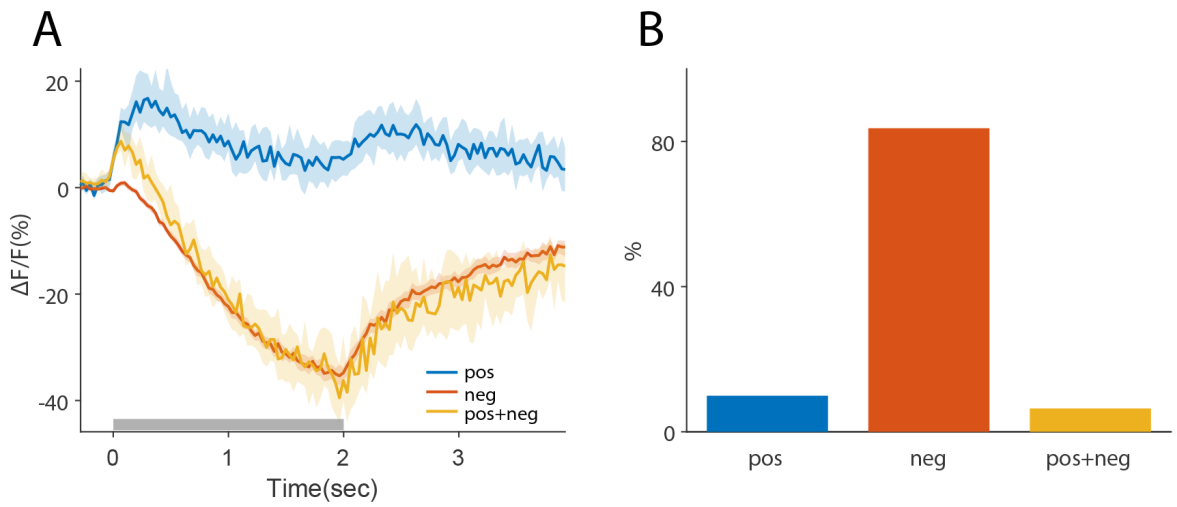

Figure S9. Related to Figure 7. Most PV cells show decerased fluorescence during tones.

(A) The responses of PV cells were classified based on the fluorescence response during the first and last 100ms of the tone in order to detect brief positive as well as suppressive responses. Cells were classified into purely positive responses, brief positive responses followed by negative responses, and purely negative responses. Shown are the average time courses of responses in each class. Shaded regions show 95% confidence interval while the gray bar indicates tones. (B) The percentage of the three responses types among significant responses. Although present, the "pos+neg" response types were rare.